

Numerical analysis of reaction forces at the supports of sliding microwire

Fazlar Rahman¹ and M. A. Salam Akanda²

¹Department of Mechanical and Production Engineering (MPE), Ahsanullah University of Science and Technology (AUST), Dhaka, Bangladesh
Phone: 88-02-8870422 Ext: 235

²Department of Mechanical Engineering, Bangladesh university of Engineering and Technology (BUET), Dhaka, Bangladesh

ABSTRACT – The reaction forces at the tungsten support probes of a platinum microwire are determined by numerical analysis for different push-pull sliding velocities and contact pressures. The Finite Element Analysis (FEA) tool ANSYS Workbench is used to evaluate the contact stresses, reaction forces and deformations of the platinum microwire. The nonlinear contact analysis and contact formulations are implemented to ensure that the platinum microwire maintained contact with the tungsten support probes during push-pull sliding motion, and transfer frictional forces between contact surfaces without penetration and separation. The reaction forces at the support probes are found independent of the sliding velocity of the platinum microwire and vary with normal contact pressure. The results found in the numerical analysis are validated through experimental works. Due to the tiny size, the nonlinearity of contacts and indeterminate supports criteria, it is difficult to determine the reaction forces at the supports of a sliding microwire by conventional mechanics. The method of the numerical analysis of the sliding microwire presented in this paper can be used to determine the reaction forces of other microstructures, validate the experimental results, as well as to evaluate total disturbance forces in the microstructures where relative motion exists; which are important for the proper design and failure analysis of the MEMS devices and microstructures.

ARTICLE HISTORY

Received: 28th Sept 2019

Revised: 28th May 2020

Accepted: 12th July 2020

KEYWORDS

Microwire;

MEMS;

finite element analysis;

frictional reaction force;

sliding microwire;

microstructure

INTRODUCTION

The MEMS (Micro-Electro-Mechanical-System) technology uses various types of microstructures to build tiny sensors, micro-actuators, micro-valves and devices [1, 2] and their size varies from 1-100 μm [3]. The microstructures are used in different forms such as wire, cantilever beam, hinge, spring, spiral, gear, and other suspended structures; which either carry the load or have mechanical functions such as deflection, displacement, deformation, rotation and relative motion, etc. [3-7]. The different types of microwires are used in MEMS technology for sensing temperature, actuation of micro-actuators, sensors, and also in the medical field for orthodontic purposes [6, 8]. The most commonly used microwire in MEMS technology is made of copper [7], NiTi [8], platinum [9], glass-coated magnetic microwire [10], silicon microwire [11, 12], aluminum, gold microwire, etc. [13]. Due to the tiny size and high surface to volume ratio of the microstructures [5], the surface driving forces such as adhesion, stiction, electrostatic, electromagnetic, piezoelectric, magnetic, etc. play an important role in the mechanical behavior of microstructures [9, 14]. As a result, the evaluation of mechanical properties, mechanical behavior, and frictional contact forces by the experimental method are quite complicated. The reaction forces at the supports of the microstructure for sliding motion depend on the type of contact surfaces, contact types, normal pressure, sliding velocity, as well as highly non-linear and unpredictable frictional properties of the contact surfaces [15, 16]. Due to the nonlinearity of the frictional contact behavior and indeterminate support criteria, it is difficult to determine the reaction forces at the supports of a sliding microwire by conventional mechanics. Also, the mechanical behavior of the microstructures in combined with the mechanical load, frictional effect, and the size scale make significant challenges to the analysis of microstructures and MEMS devices [17]. These challenges are possible to overcome by using Finite Element Analysis (FEA) tools such as ANSYS, IDEAS, ABAQUS, COSMOS, etc. [18, 19]. The fatigue life, reliability, performance and response of the MEMS devices depend on the contact forces, as well as the mechanical behavior of microstructures [3]. Hence, it is vital to find the reaction forces between the sliding microstructures and their supports. Without finding the reaction or contact forces between the microstructures and supports [6], the proper design and evaluation of the performance of MEMS devices and sensors are not possible [3, 9]. For example, the manipulation of a microwire is challenging and difficult without knowing the contact frictional forces between the microwire and gripper to pick up the microwire from the substrate fabricated by Electromigration [13].

Many remarkable studies [5-8, 17, 18, 20-22] are reported on the Finite Element Analysis (FEA) of different types of microstructures such as beam, bridge, flexible hinge, wire, membrane and carbon nanotube. Still, there is a significant lack of works on Finite Element Analysis (FEA) of sliding microstructures of the MEMS such as microwire, microrod, microbar, etc. In our best knowledge, none of the studies is being reported yet on the FEA of sliding microwire. The

objective of this study is to determine the contact stress, reaction forces, and deformation of the sliding platinum microwire against two opposite tungsten support probes for various push-pull sliding velocities and contact pressures using numerical analysis tool ANSYS Workbench.

METHODOLOGY

The reaction forces at the supports of the microwire for push-pull sliding motions are difficult to evaluate by conventional mechanics, because of the nonlinearity of contact behavior, indeterminate support criteria, and size scale of the microstructures. It is required to solve and simulate the contact problem numerically by using Finite Element Analysis (FEA) tools [18]. The contact problems are nonlinear, and the degree of nonlinearity depends on the shape and geometry of the contact surfaces, coefficient of friction, boundary conditions, contact type and normal load [23]. The geometric and frictional nonlinearity makes the numerical analysis of contact problems harder to simulate and converge [23]. The FEA tool ANSYS Workbench is used to solve the contact problem between a sliding microwire and two opposite support probes. In this study, only static coefficient of friction $\mu_s = 0.23$ [9] between the contacts surfaces of the microwire and support probes are incorporated in the numerical analysis for simplification. The numerical analysis of the contact problem includes the geometry of microstructures, contact detection and formulation, material properties, meshing, boundary conditions and load, and setting of the analysis, which are presented in the subsequent paragraphs.

Model Geometry

The geometry of the model includes a $0.625 \mu\text{m}$ diameter and $65 \mu\text{m}$ long platinum microwire, two tungsten support probes of $5.0 \mu\text{m}$ diameter, and a $22.75 \mu\text{m}$ long steel Double Beam Cantilever (DBC) of $1.10 \mu\text{N}/\mu\text{m}$ stiffness. The geometric configuration is kept similar to the experiment available in the literature to ensure the justification of comparison and conformity with the experimental results [9]. The geometric configuration used in this work for numerical analysis is shown in Figure 1(b) and a similar experimental setup [9] shown in Figure 1(a).

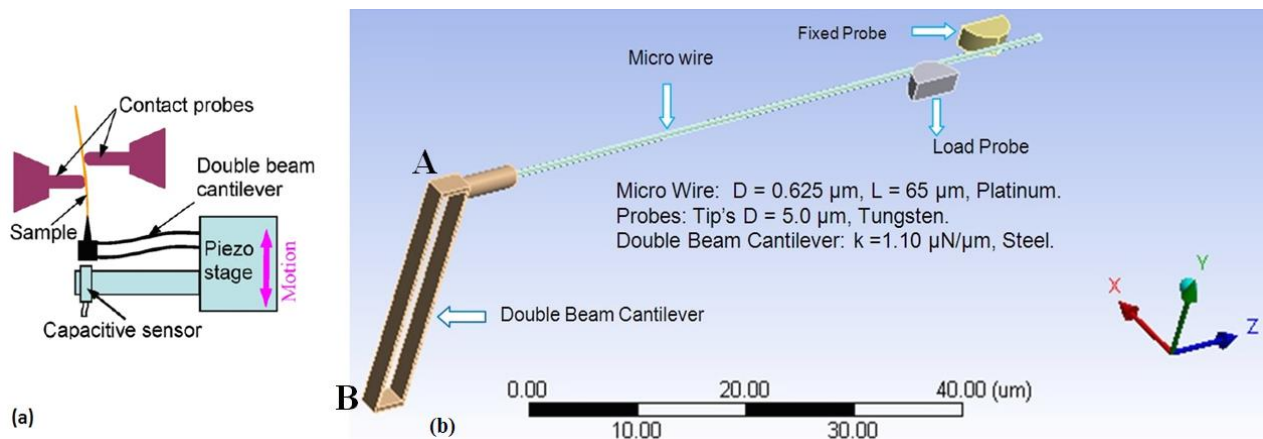


Figure 1. (a) Schematic of experimental setup [9] and (b) Geometry of the setup used in numerical analysis

In the experimental setup, one end of the platinum microwire is attached to the Double Beam Cantilever (DBC) by Joule heating [24] and another end of the DBC is attached to the Piezo-Stage. The linear displacement of the Piezo-Stage induces the linear sliding motion to the platinum microwire against the tungsten support probes. The farthest support probe from the DBC is fixed and the other probe refers to 'load probe' which is free to move only along the lateral direction of the microwire. The distance between the load and fixed probes is $10 \mu\text{m}$. The Double Beam Cantilever (DBC) is built by two identical simple cantilever beams of thickness $0.25 \mu\text{m}$ and width $2.0 \mu\text{m}$, where the ends are connected to a fixed support, which provides no changing of slopes at the two ends during bending and transferring the load to each other [25]; and also provide the benefit of linear actuation without in-plane bending of the microwire during push-pull sliding motions against support probes. The stiffness of the DBC is determined by Finite Element Analysis and also validated by the following equation [26],

$$k = \frac{24 \times E \times I}{L^3} \quad (1)$$

where E = Modulus of elasticity of the beam material, L = length of the beam and I = moment of inertia of the single simple cantilever beam.

ANSYS Workbench is used for 3D modeling of the microwire, support probes and Double Beam Cantilever (DBC). The round portions of the support probes are modeled and meshed only to reduce the number of elements and run time of the numerical analysis.

Contact Detection and Formulation

The numerical analysis of the sliding platinum microwire against the two opposite tungsten support probes is a frictional contact analysis. There are two significant difficulties in solving contact problems. First, the behavior of contact surfaces is unpredictable and uncertain [17, 23]. Depending on the boundary conditions, load and surface type, the contact surfaces may penetrate or separate from each other without transferring the load and converging the solution [15]. Second, the frictional response is nonlinear and chaotic which intensifies the difficulties in the convergence of the contact problem [15]. To solving contact problems, the identification of contact surfaces, contact pairs, contact types and contact formulation are very important. In this work, two pairs of surface-to-edge frictional contacts are used between the microwire and support probes with a coefficient of friction 0.23 [9]; and the left end of the microwire is bonded to the Double Beam Cantilever (DBC). The cylindrical surface of the microwire is treated as target and the edges of the probes are treated as contact surfaces. The auto-asymmetric contact and Pure Penalty method are used for contact formulation and convergence of the numerical solution.

Material Properties

The microwire, support probes and Double Beam Cantilever (DBC) are made of platinum, tungsten and steel respectively. Due to the special fabrication process and techniques, the microstructures have fewer defects and higher mechanical strengths than the bulk materials [27]. Therefore, the material properties of the bulk materials can't be applied directly to the microstructure. In this work, the linear elastic properties of the material of microwire, microprobe and DBC are obtained from the relevant research papers of microstructures [9, 25]. The linear elastic properties of the materials are shown in Table 1.

Table 1. Materials properties

| Microstructure | Material | Modulus of Elasticity E (MPa) | Poisson's Ration, ν | Density ρ (kg/ μm^3) |
|------------------------|----------|-------------------------------|-------------------------|---------------------------------------|
| Double Beam Cantilever | Steel | 2.07×10^5 | 0.30 | 7.85×10^{-15} |
| Microwire | Platinum | 1.76×10^5 | 0.39 | 2.145×10^{-14} |
| Support Probes | Tungsten | 4.0×10^5 | 0.28 | 1.96×10^{-14} |

Meshing

The accuracy, convergence and solution speed of the Finite Element Analysis (FEA) greatly depends on the meshing and type of element. The solid geometry of the microwire and Double Beam Cantilever (DBC) are meshed with Patch conforming and the support probes with Hex dominant meshing algorithm. The contact elements CONTA175, CONTA174 and target element TARGE170 are used in the meshing of underlying contact surfaces. The solid geometry of the microwire, probes, and DBC are meshed with 52,027 numbers of higher-order 3D solid elements including 20 nodes Hexahedrons, 10 nodes Tetrahedral, 13 nodes Pyramid and 15 nodes Wedge with advance size function and shape checking option. The meshing of the model is shown in Figure 2. The mesh density is checked by the mesh independency test of maximum contact stress in the platinum microwire, which is shown in Figure 3.

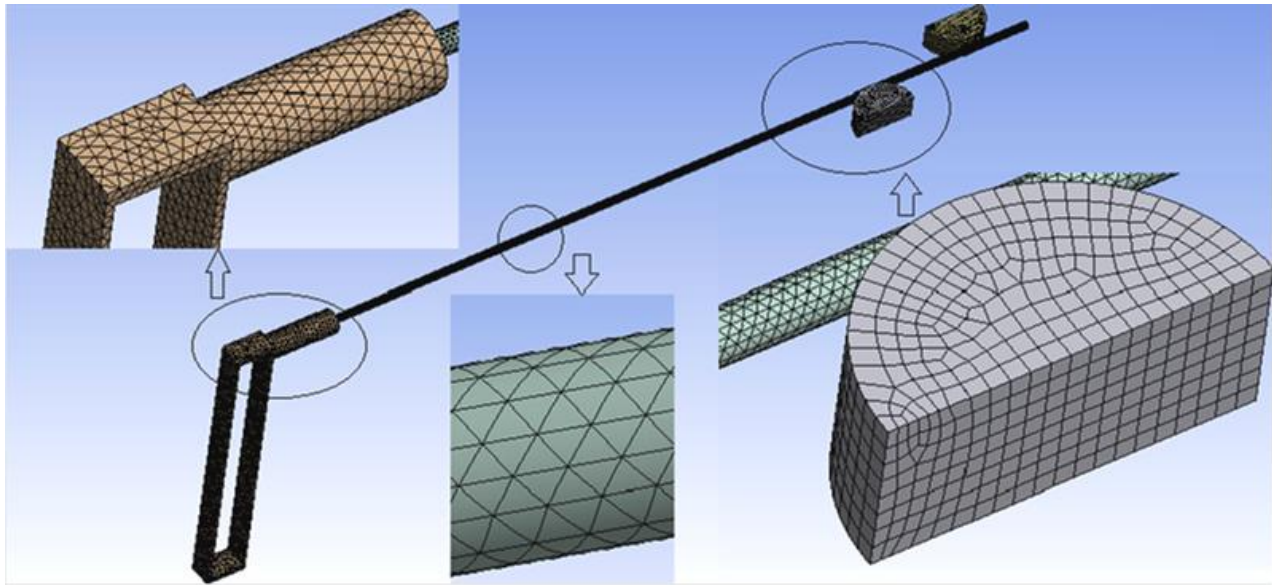


Figure 2. Meshing of microwire, support probes and double beam cantilever

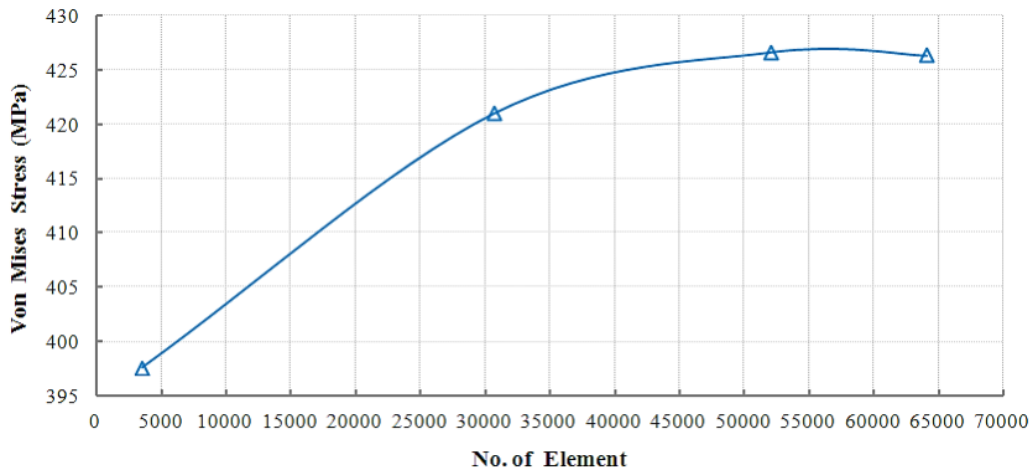


Figure 3. Mesh independency test on maximum contact stress in the microwire

Boundary Conditions and Load

The boundary conditions and load are the most important part of the Finite Element Analysis (FEA). It ensures proper behavior and deformation of the microstructures, accuracy of the solution, as well as simulation of the actual phenomena. In this study, the appropriate boundary conditions are used in the model to implement the contact compatibility between the microwire and support probes — the microwire will not penetrate or separate from the contact surfaces while sliding motion and transferring the load to each other; as well as simulate the push-pull sliding motions of the microwire available in the experimental study [9]. The similar boundary conditions of the experimental study [9] are used in the numerical analysis for justifying the comparison and validation of the results.

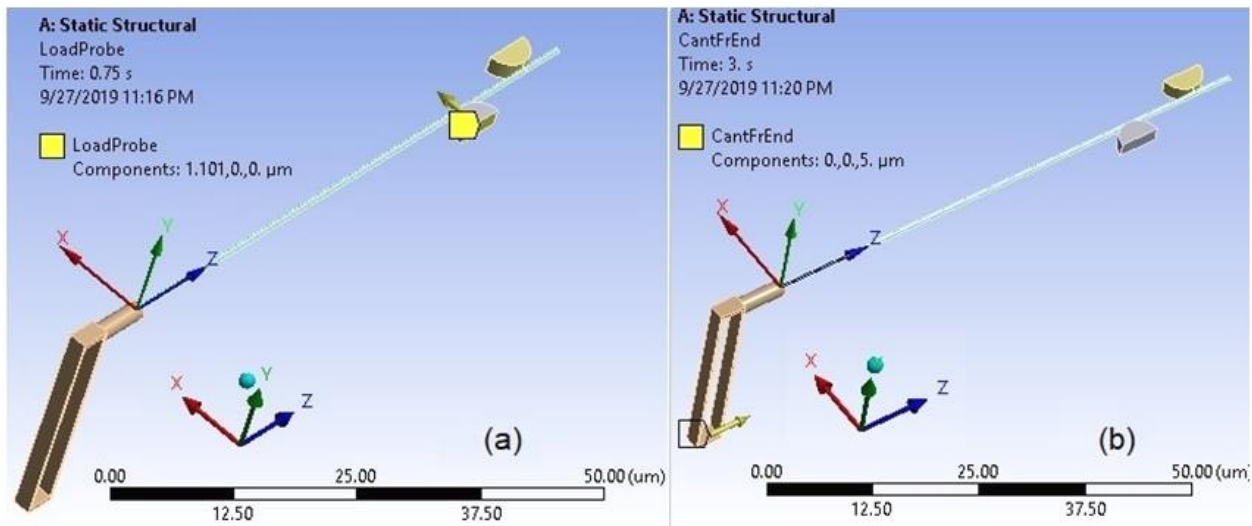


Figure 4. Displacement of: (a) load probe along X-direction and (b) end 'B' of DBC along Z-direction

The load probe is free to move only along the lateral direction (along X-axis) of the microwire, Figure 4(a). The farthest probe refers to 'fixed probe' and works like fixed support where the microwire is supported by static frictional force only. The end 'B' of the Double Beam Cantilever (DBC) is free to move only along the longitudinal direction (along Z-axis) of the microwire, which represents the linear displacement of the Piezo-Stage in the experimental setup [9], Figure 4(b). A fixed lateral displacement (along X-direction) is applied at the load probe before applying the displacement at the end 'B' of the DBC to generate normal pressure at the contact surfaces. Due to the stiffness of the DBC, the microwire is started to slide when the force applied through the displacement of the end 'B' overcomes the frictional force at the contact surfaces. Before starting the sliding motion of the microwire, the elastic bending force in the microwire is balanced by the static frictional resistive force. During the sliding motion, the elastic bending force is balanced by the kinetic frictional resistive force at the contact surfaces.

Before starting the sliding motion of the microwire, a fixed displacement of 1.10 μm is applied along X-direction at the load probe between 0 to 0.75 seconds to generate contact pressure at the support probes. Then, the push and pull sliding motions are applied to the microwire by applying a linear displacement at end 'B' of the Double Cantilever Beam (DBC) along Z-direction between 1.0 to 3.0 seconds and 4.0 to 6.0 seconds respectively. The microwire remains in static condition from 3.0 to 4.0 seconds and also from 6.0 to 6.98 seconds.

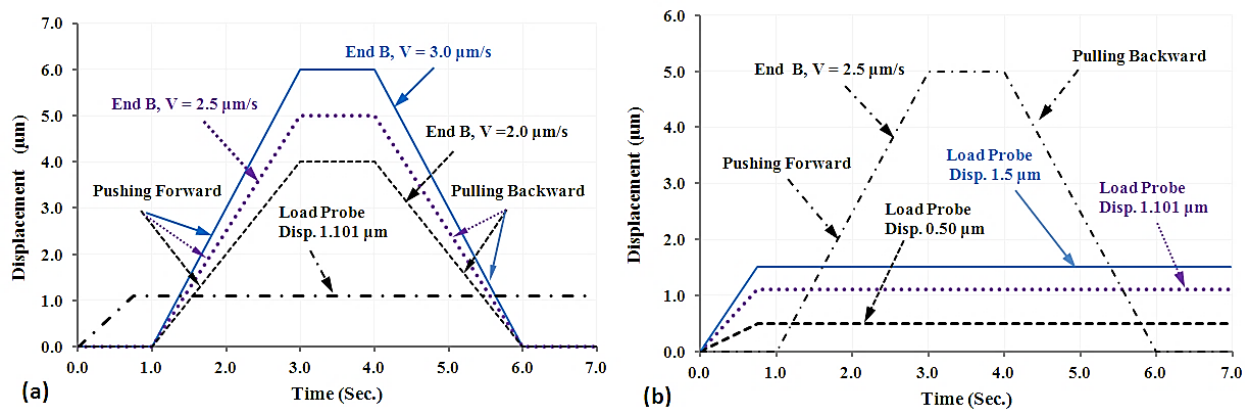


Figure 5. (a) First set of B.C. and (b) Second set of B.C. (V = Applied motion at end 'B' of DBC and load probe displacement in X-direction)

In this study, the reaction forces at the support probes of the sliding microwire are determined for the two sets of boundary conditions, which are shown in Figure 5. In the first set, the displacement at the end 'B' of the Double Beam Cantilever (DBC) is applied along Z-axis for three different linear velocities of 3.0 μm/s, 2.50 μm/s and 2.0 μm/s with a constant lateral displacement of 1.101 μm to the load probe, Figure 5(a). In the second set, three different lateral displacements of 0.50 μm, 1.101 μm, and 1.50 μm are applied to the load probe with a linear sliding velocity 2.50 μm/s at the end 'B' of the DBC, Figure 5(b).

Setting of Analysis

Using multiple load steps allows solving the numerical analysis sequentially for several loads. In the nonlinear analysis, the loads in each load step are applied gradually over time, which helps to achieved and enhances the convergence of the solution with higher accuracy [28], although it increases the solution time. The load in each time step is divided into a number of sub-steps based on time or load history. The smaller time step size converges the solution easier, however, it requires more computing resources and solution time [28]. In this work, the entire load time history (0 to 6.98 seconds) is divided into 6-time steps, which is shown in Figure 6. The non-linear solution with 6-time steps and direct solver option is used with 320 initial, 180 minimum and 650 numbers of maximum sub-steps in each time step to converge the solution. It required 18 hours of solution time to complete the simulation using the hardware resources of Intel 4 core i7-7500U @ 2.70 GHz CPU, 4GB graphics memory and 16 GB RAM on Hp Pavilion Laptop.

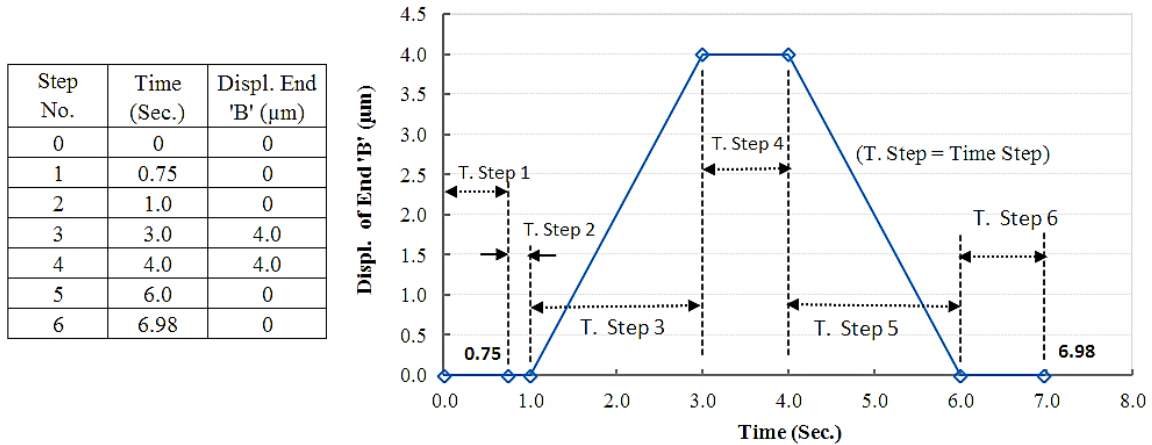


Figure 6. Number of time steps setting in analysis

RESULTS AND DISCUSSION

Contact Stress

The maximum contact stresses are found 426.76 and 582.82 MPa in the platinum microwire for the first and second sets of boundary conditions respectively, which is shown in Figure 7. It is also found that for a constant contact pressure or displacement of the load probe, the contact stress remains independent of the sliding velocity of microwire (Figure 8(a)); and for a constant sliding velocity of the microwire, the contact stress increases linearly with contact pressure (Figure 8(b)), which agrees with the principle of friction and justify the accuracy of the solution.

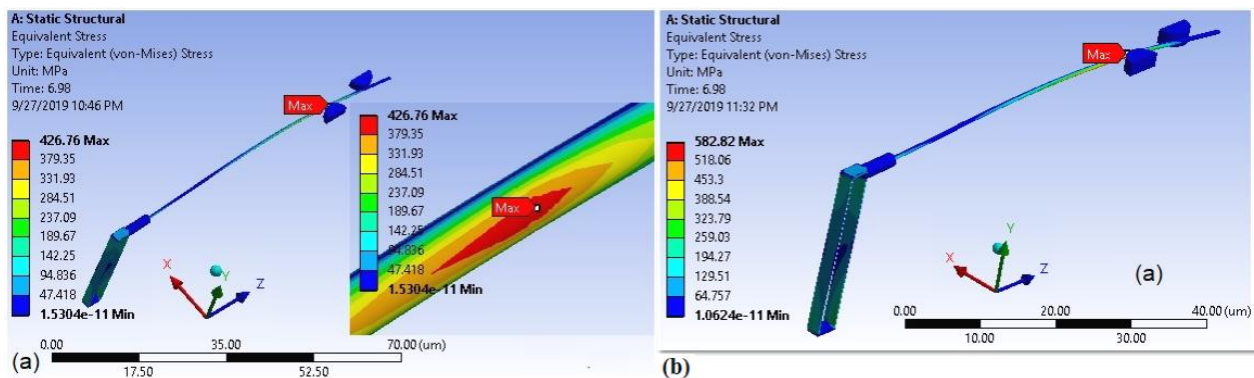


Figure 7. Maximum contact stress in microwire for: (a) first set of B.C. and (b) second set of B.C.

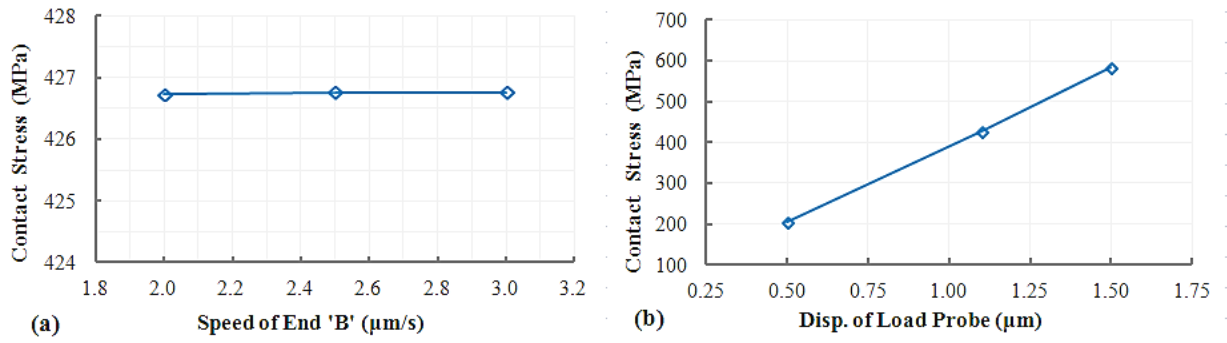


Figure 8. Contact stress: (a) independent of sliding velocity (first set of B.C.) and (b) increases with contact pressure (second set of B.C.)

Reaction Force

First Set of Boundary Conditions

The tangential and normal reactions forces at the support probes of the platinum microwire for a fixed contact pressure and three different sliding velocities are shown in Figure 9 and Figure 10.

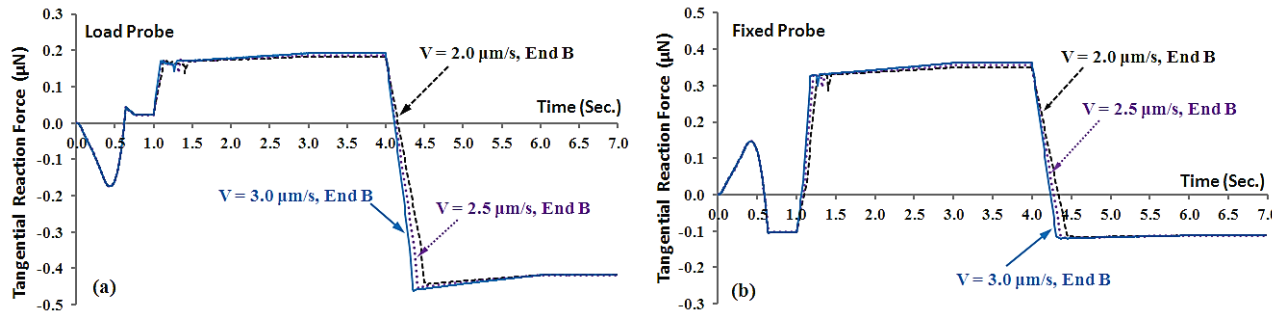


Figure 9. Tangential reaction force at: (a) load probe and (b) fixed probe

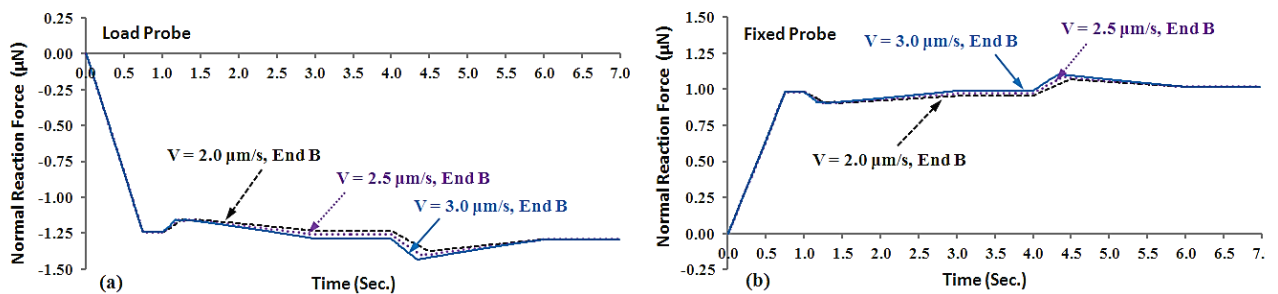


Figure 10. Normal reaction force at: (a) load probe and (b) fixed probe

The tangential reaction forces at the load and fixed probe have the same pattern for all three different sliding velocities from 1.0 second to 6.98 seconds. During 0 to 0.75 second, the normal contact pressure is applied to the microwire through a fixed displacement (1.101 μm) of the load probe in the lateral direction. As a result, small tangential reaction forces are developed in both probes due to the surface friction and relative slip between the probes and microwire. During 0 to 0.75 second, the tangential forces in the support probes are opposite to each other since probes located on the opposite side of the microwire. Before starting the sliding motion of the microwire, the constant normal forces of 1.244 and 0.98 μN are also developed in the contact surfaces of load and fixed probes respectively from 0.75 to 1.0 second, Figure 10. The normal reactions forces at the load and fixed probes are also opposite to each other because the probes are located at the opposite side of the microwire.

The patterns of the tangential and normal reaction forces in the load and fixed probes remain almost the same for all three sliding velocities (2.0, 2.5 and 3.0 $\mu\text{m/s}$) of end 'B' of the Double Beam Cantilever (DBC). For a constant pressure at contact surfaces, the reaction forces at the support probes are remained independent of sliding velocity of the microwire.

Second Set of Boundary Conditions

The tangential and normal reaction forces at the support probes of the platinum microwire for a constant sliding velocity and three different contact pressures are shown in Figure 11 and Figure 12, respectively.

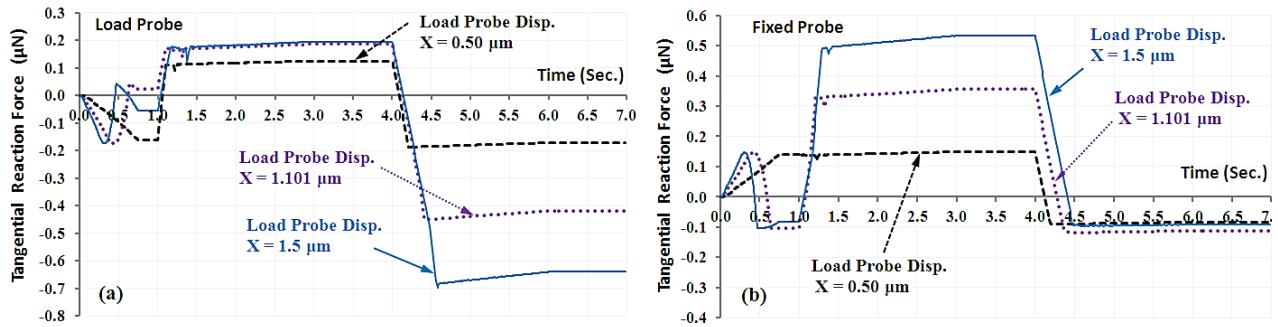


Figure 11. Tangential reaction force at: (a) load probe and (b) fixed probe

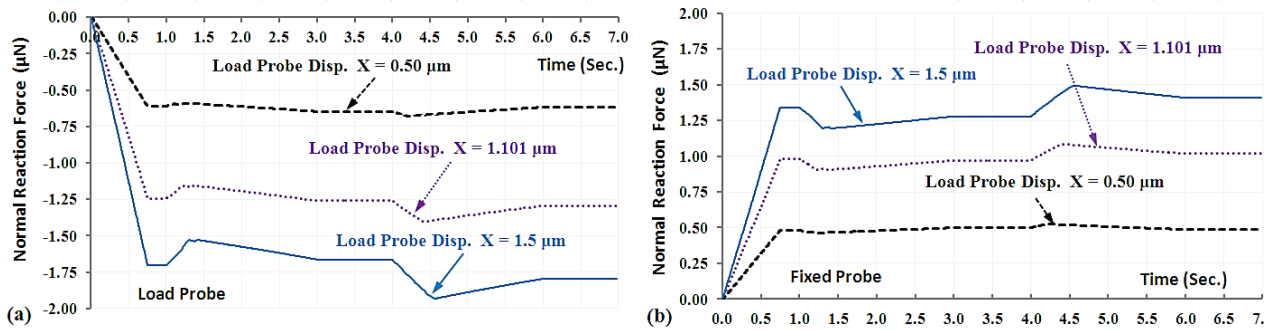


Figure 12. Normal reaction force at: (a) load probe and (b) fixed probe

The tangential and normal reaction forces at the load and fixed probes are increased with contact pressure or lateral displacement of the load probe. The reaction forces are the highest for the highest contact pressure and lowest for the lowest contact pressure, which agrees with the principle of friction. Due to the increase of contact pressure, the frictional resistive forces at the contact surfaces are also increased, as a result, the higher force/displacement is required to apply at the end 'B' of the Double Beam Cantilever (DBC) to overcome the frictional resistive force at the support probes. Due to the higher applied force, as well as the higher resistive force, the microwire bent more along the lateral direction due to increasing of the contact pressure. It is noted that an infinitesimal amount of reaction forces are developed at the probes along Y-direction in both sets of boundary conditions, which are neglected and not presented. It also indicates the accuracy of the numerical analysis.

Deformation of Microwire

First Set of Boundary Conditions

The sliding distance of the platinum microwire along longitudinal direction (along Z-axis) and the lateral deflection (along X-axis) for a fixed pressure and three sliding velocities are shown in Figure 13. The location and magnitude of the maximum lateral deformation of the microwire for three sliding velocities are shown in Figure 14.

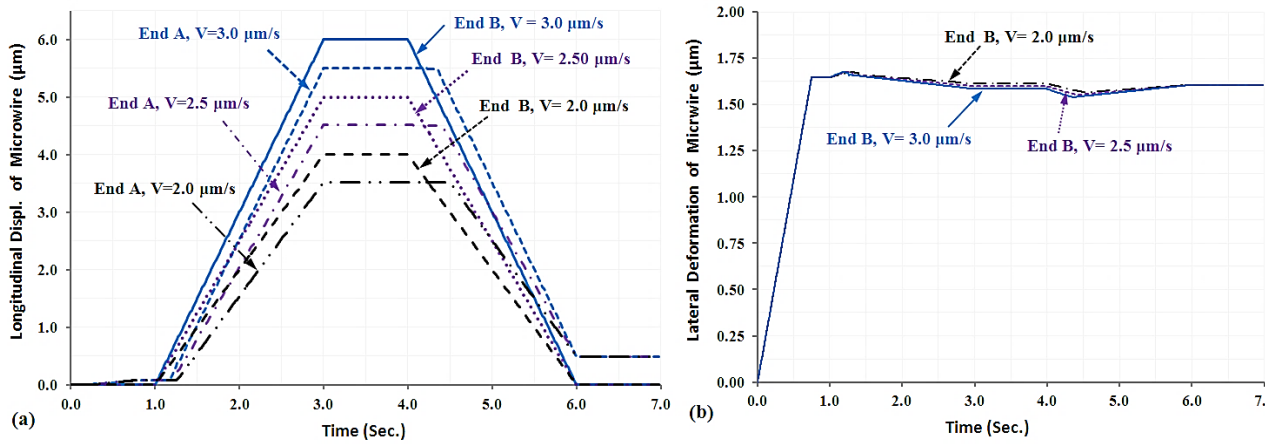


Figure 13. (a) Longitudinal sliding distance and (b) Lateral deflection of microwire

The push-pull sliding distance of the platinum microwire along the longitudinal direction is found by evaluating the distance along Z-direction of the end 'A' of Double Cantilever Beam (DBC). The sliding distance of the microwire along the longitudinal direction increases with the linear motion applied at the end 'B' of DBC for a constant contact pressure or fixed lateral displacement of the load probe. The microwire slides through 5.503, 4.514 and 3.523 µm for the velocities of 3.0, 2.5 and 2.0 µm/s applied at the end 'B' of DBC. During the forward sliding motion of microwire, the end 'A' of the DBC always remained behind of end 'B'. This is happened due to the stiffness of the DBC and frictional resistive force at the contact surfaces of the microwire and probes. The microwire is started to slide when the force applied through the displacement of the end 'B' of DBC overcomes the frictional resistive forces at contact surfaces. Before sliding of the microwire, the frictional resistive forces at the contact surfaces are balanced by the elastic bending force of the microwire, as a result, it deforms along the lateral direction. Due to the same reason, the end 'B' of DBC remains ahead of the end 'A' during backward motion of the microwire from 4.0 to 6.0 seconds; and the end 'A' remains off by 0.493 µm at 6.0 seconds, although the end 'B' returns to the initial position. At this point, the microwire remains in static condition by deforming in the lateral direction by 1.606 µm, Figure 13(b). During sliding motion, the elastic bending force in the microwire is balanced by the kinetic frictional force at the contact surface of the support probes. The microwire slides along the longitudinal direction by a negligible amount for the time step 0 to 0.75 seconds, through which the load probe is pushed along the lateral direction to generate contact pressure.

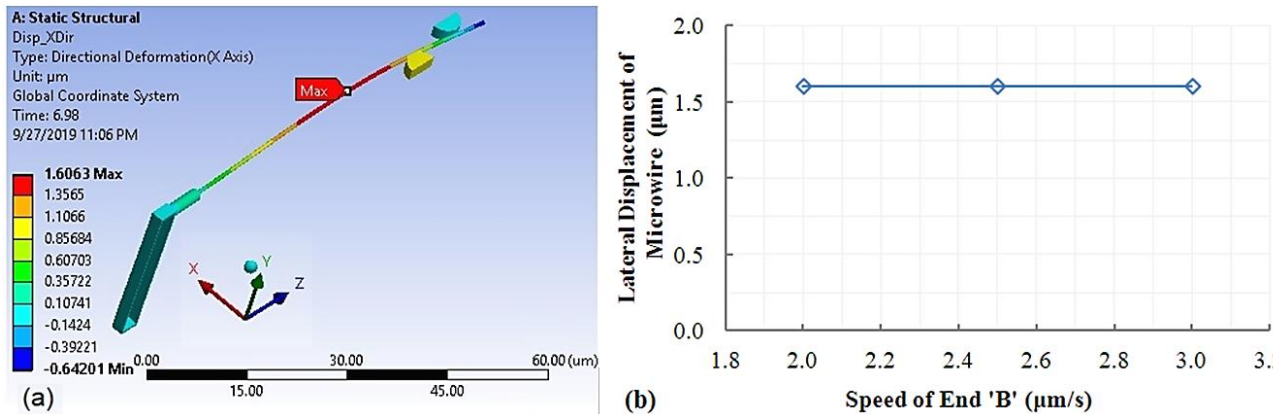


Figure 14. (a) Maximum lateral deformation and (b) Lateral deformation against sliding velocity of microwire

The lateral displacement of the microwire along X-direction increases linearly up to 0.75 seconds and remains constant up to 1.0 second, and then decreases gradually up to 4.0 seconds, Figure 13(b). It is also increasing gradually during the pullback motion of the microwire from 4.0 seconds to 6.0 seconds. The lateral displacement of the microwire remains constant from 3.0 to 4.0 seconds and from 6.0 to 6.98 seconds since there is no sliding motion of the microwire. The maximum lateral deflection of the microwire is found 1.606 µm at a point between the load probe and left end of the microwire, which is shown in Figure 14(a). For a constant contact pressure, the lateral deflection of the microwire is also found independent of the sliding velocity, which is shown in Figure 14(b) and agrees with the principle of friction.

Second Set of Boundary Conditions

The sliding distance of the platinum microwire along the longitudinal direction (along Z-axis) and the lateral deflection (along X-axis) for three different contact pressures with a constant sliding velocity are shown in Figure 15. The location and magnitude of the maximum lateral deformation of the microwire for the same boundary conditions are shown in Figure 16.

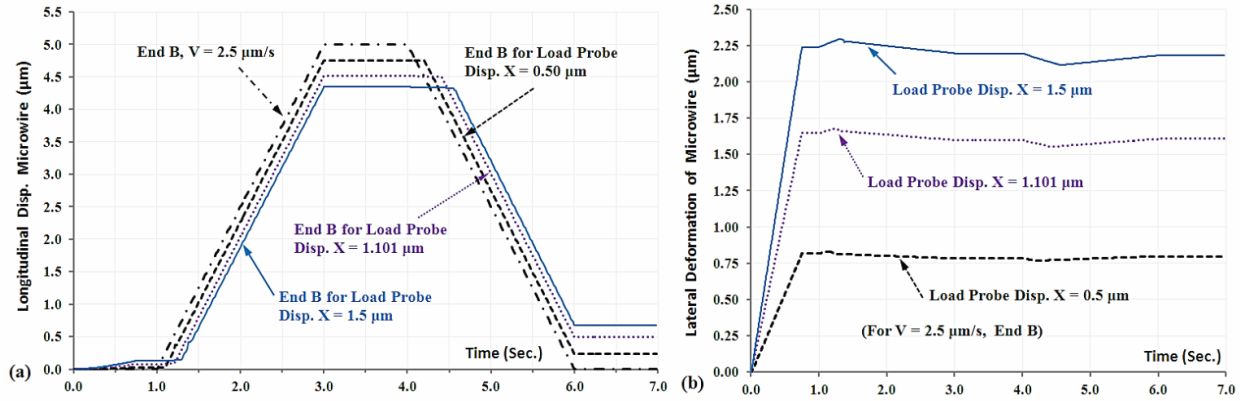


Figure 15. (a) Longitudinal sliding distance and (b) Lateral deflection of microwire

The sliding distance and lateral deformation of the microwire are found to be the similar fashion of the first set of load conditions. However, the longitudinal displacement of the left end of the microwire is the highest for the lowest contact pressure or lowest lateral displacement of 0.50 µm of the load probe, and the lowest for the highest lateral displacement of 1.5 µm of the load probe. The sliding distance of the microwire is also the highest for the lowest contact pressure and vice versa, which agrees with the principles of friction because the tangential frictional force varies directly with the normal force at the contact surface (Figure 15).

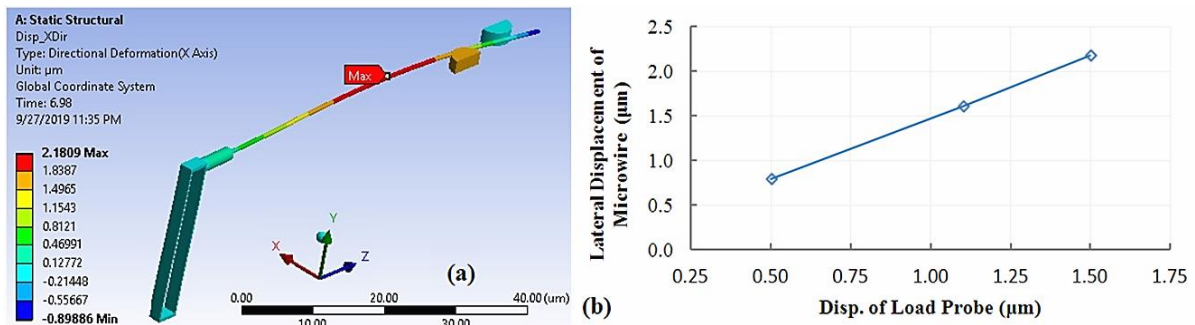


Figure 16. (a) Lateral deformation and (b) Lateral displacement against contact pressure of microwire

The maximum lateral deflection of the microwire is found at a point between the load probe and left end of the microwire, Figure 16(a). The maximum lateral deflection of 2.181 µm is found for the highest contact pressure or the highest lateral displacement of 1.50 µm of the load probe. The lowest lateral deflection of 0.7981 µm is found for the lowest contact pressure of 0.50 µm, which is shown in Figure 16(b). For a fixed sliding velocity, the lateral deflection of the microwire increases with the contact pressure and vice versa, which agrees with the principle of friction. Because the higher contact pressure generates higher tangential frictional force at the contact surfaces, which resists the sliding motion of the microwire robustly. As a result, the higher force/displacement is required to apply at the end 'B' of the Double Beam Cantilever (DBC) to overcome the resistive frictional force, and it leads the microwire to deflect more along the lateral direction.

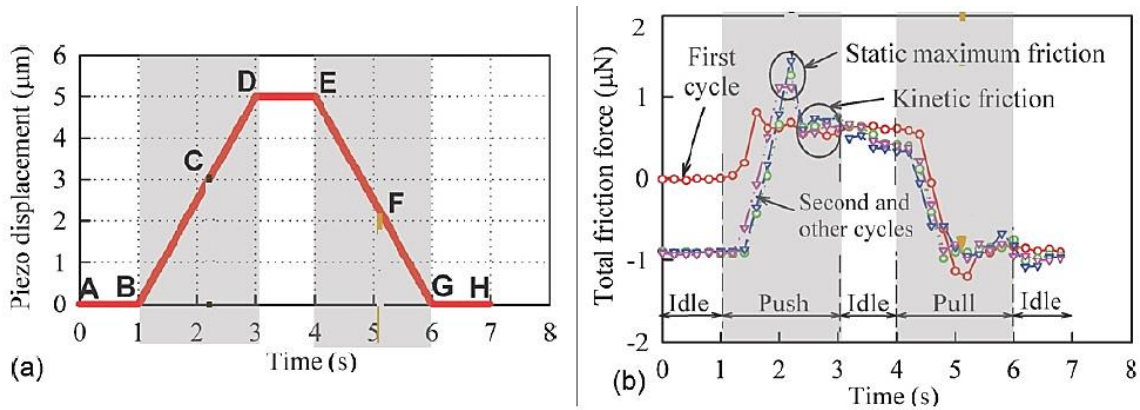


Figure 17. (a) Displacement of piezo-stage (end 'B' of DBC) and (b) Total frictional Force in microwire [9]

The graphs of the applied displacement at the end 'B' of the Double Beam Cantilever (DBC) and the total tangential frictional force found in the microwire in experimental work [9] are shown in Figure 17(a) and Figure 17(b) respectively. The total frictional force in the microwire is the algebraic summation of the tangential frictional forces at the load and fixed probes. In both sets of load cases, the pattern of the graphs of the tangential reaction forces at the load and fixed probes are found similar to the graph of the experimental work, Figure 17(b); which indicates the accuracy and appropriateness of the numerical analysis presented in this paper. In both sets of boundary conditions, an infinitesimal and negligible amount of reaction forces are developed at the probes along Y-direction during the sliding motion of the microwire. It also signifies the accuracy of the numerical analysis since no external force is applied along the vertical direction or Y-axis of the model. The experimental work is done for multiple cycles of push-pull motions of the microwire and in the presence of disturbance forces from the surroundings. In addition, the surface asperities on the microwire and probes, which also play vital role in the contact behavior. However, the numerical analysis is done in the absence of all disturbance forces, surface asperities, and also using the similar boundary conditions of the experimental study. Therefore, some deviations of results of the numerical analysis from the experimental are acceptable.

CONCLUSIONS

The reaction forces at the support probes of the sliding microwire remain independent of the sliding velocity for constant contact pressure. The tangential reaction force at the support probes and lateral deflection of the microwire increase with contact pressure if sliding velocity remains constant, which agrees with the principle of friction of the bulk material. The procedure and method of the numerical analysis presented in this paper can be used to determine the contact behavior and reaction forces at the supports of other microstructures where relative motion exists. It will also facilitate the evaluation of the design, deformation, response, and performance of the MEMS devices and microstructures without experiment. Although the experiment of the microstructures and MEMS's devices is performed in a controlled environment, it is still difficult to minimize the disturbance forces entirely due to the tiny size and high surface to volume ratio. The numerical analysis method presented in this paper can be used as an alternative to the experiment and the validation of the experimental results. Since numerical analysis is done in the absence of all disturbance forces, the results of this study can be applied to quantify the total disturbance forces in the microwire by finding the differences between the results of the numerical analysis and experimental.

ACKNOWLEDGMENTS

The authors gratefully acknowledge the Department of Mechanical and Production Engineering (MPE) of Ahsanullah University of Science and Technology (AUST), Dhaka, Bangladesh, for supporting this work and also Bangladesh University of Engineering and Technology (BUET), Dhaka, Bangladesh, for funding.

REFERENCES

- [1] TechnologyWatch, *An Introduction to MEMS (Micro-electromechanical Systems)*. Loughborough University, UK: PRIME Faraday Partnership, 2002.
- [2] "What is MEMS Technology," https://www.memsnet.org/mems/what_is.html, 2018 [Online].
- [3] T. Buchheit, B. Boyce, and G. Wellman, "The role of microstructure in MEMS deformation and failure," in *ASME 2002 International Mechanical Engineering Congress and Exposition*, 2002, pp. 559-566.

- [4] T. M. Adams and R. A. Layton, "MEMS transducers—An overview of how they work," in *Introductory MEMS*, ed: Springer, 2010, pp. 167-210.
- [5] J. K. Sakellaris, "Finite element analysis of micro-Electro-Mechanical systems: Towards the integration of MEMS in design and robust optimal control schemes of smart microstructures," *WSEAS Transactions on Applied and Theoretical Mechanics*, pp. 114-124, 2008.
- [6] M. Pustan, S. Paquay, V. Rochus, and J.-C. Golinval, "Modeling and finite element analysis of mechanical behavior of flexible MEMS components," *Microsystem Technologies*, vol. 17, pp. 553-562, 2011.
- [7] Q.-S. Bai, K. Cheng, B. He, and Y.-C. Liang, "Design of a novel tensile testing device and its application in tensile testing experiments on copper micro wires," *Proceedings of the Institution of Mechanical Engineers, Part B: Journal of Engineering Manufacture*, vol. 226, pp. 1594-1600, 2012.
- [8] M. Razali, A. Mahmud, N. Mokhtar, and J. Abdullah, "Finite-element analysis of NiTi wire deflection during orthodontic levelling treatment," in *IOP Conference Series: Materials Science and Engineering*, 2016, p. 012040.
- [9] M. S. Akanda, H. Tohmyoh, and M. Saka, "Precision friction measurement between ultrathin wire and microprobe," *Sensors and Actuators A: Physical*, vol. 172, pp. 189-194, 2011.
- [10] S. A. Baranov, V. S. Larin, and A. V. Torcunov, "Technology, preparation and properties of the cast glass-coated magnetic microwires," *Crystals*, vol. 7, p. 136, 2017.
- [11] T. Tsuchiya, T. Hemmi, J.-y. Suzuki, Y. Hirai, and O. Tabata, "Tensile strength of silicon nanowires batch-fabricated into electrostatic MEMS testing device," *Applied Sciences*, vol. 8, p. 880, 2018.
- [12] D. L. Chandler, "New way to grow microwires," ed. MIT News Office, 2011.
- [13] H. Tohmyoh, M. Abdus Salam Akanda, and Y. Nobe, "Mechanical properties of thin Al wires prepared by electromigration," *Journal of the Physical Society of Japan*, vol. 81, p. 094803, 2012.
- [14] J. Biener, A. V. Hamza, and A. Hodge, "Deformation behavior of nanoporous metals," in *Micro and nano mechanical testing of materials and devices*, ed: Springer, 2008, pp. 118-135.
- [15] "Contact Technology Guide Release 12.1," *ANSYS Inc.*, 2009.
- [16] "Introduction to ANSYS Mechanical: Modeling Connection Release 15.0 " *ANSYS Inc*, 2012.
- [17] G. Ulises, "Modeling and simulating MEMS devices using finite element analysis," in *Proceedings of 2001 ASME International Mechanical Engineering Congress and Exposition, New York, NY, United States*, 2001, pp. 2583-2587.
- [18] H. Ren and J. Yao, "FEA in Micro-Electro-Mechanical Systems (MEMS) Applications: A Micromachined Spatial Light Modulator (μ SLM)," *Finite Element Analysis: New Trends and Developments*, pp. 161-182, 2012.
- [19] W. A. Siswanto, M. Nagentrau, and A. L. Mohd Tobi, "Prediction of residual stress using explicit finite element method," *Journal of Mechanical Engineering and Sciences*, vol. 9, pp. 1556-1570, 2015.
- [20] J. Wikström, "Finite element simulations of microbeam bending experiments," 2017.
- [21] F. Golesorkhie and M. Navi, "Effects of geometric variations on buckling properties of carbon nanostructures: A finite element analysis," *Journal of Mechanical Engineering and Sciences*, vol. 14, pp. 6473-6487, 2020.
- [22] B. Xu, B. Zhao, and Z. Yue, "Finite element analysis of the indentation stress characteristics of the thin film/substrate systems by flat cylindrical indenters," *Materialwissenschaft und Werkstofftechnik: Entwicklung, Fertigung, Prüfung, Eigenschaften und Anwendungen technischer Werkstoffe*, vol. 37, pp. 681-686, 2006.
- [23] R. P. Barrett, "ANSYS Nonlinear Convergence Best Practices," *CAE Associates*, 2012.
- [24] H. Tohmyoh, M. S. Akanda, and M. Saka, "Small-span bending test for determination of elastic-plastic properties of ultrathin Pt wires," *Applied Physics A*, vol. 103, pp. 285-291, 2011.
- [25] M. A. S. Akanda, H. Tohmyoh, and M. Saka, "An integrated compact unit for wide range micro-Newton force measurement," *Journal of Solid Mechanics and Materials Engineering*, vol. 4, pp. 545-556, 2010.
- [26] M. C.-Y. Niu, "Airframe stress analysis and sizing," *Hong Kong Conmlit Press Limited*, 1997.
- [27] F. Yang and J. C.-M. Li, *Micro and nano mechanical testing of materials and devices*: Springer, 2008.
- [28] H.-H. Lee, *Finite Element Simulations with ANSYS Workbench 2019*: SDC Publications, 2019.